Defect mechanisms in high resistivity $BaTiO_3$–$Bi(Zn_{1/2}Ti_{1/2})O_3$ ceramics

Natthaphon Raengthon,[1] Victoria J. DeRose,[2] Geoffrey L. Brennecka,[3] and David P. Cann[1]
[1]*Materials Science, School of Mechanical, Industrial, and Manufacturing Engineering, Oregon State University, Corvallis, Oregon 97331, USA*
[2]*Department of Chemistry, University of Oregon, Eugene, Oregon 97403, USA*
[3]*Sandia National Laboratories, Materials Science and Engineering Center, Albuquerque, New Mexico 87185, USA*

(Received 20 June 2012; accepted 29 August 2012; published online 13 September 2012; publisher error corrected 14 September 2012)

The defect mechanisms that underpin the high energy density dielectric $0.8BaTiO_3$–$0.2Bi(Zn_{1/2}Ti_{1/2})O_3$ were investigated. Characterization of the nominally stoichiometric composition revealed the presence of a Ti^{3+}-related defect center, which is correlated with lower resistivities and an electrically heterogeneous microstructure. In compositions with 2 mol. % Ba-deficiency, a barium vacancy-oxygen vacancy pair $(V_{Ba} - V_O)$, acted as an electron-trapping site. This defect was responsible for a significant change in the transport behavior with a high resistivity and an electrically homogeneous microstructure. © *2012 American Institute of Physics*. [http://dx.doi.org/10.1063/1.4752452]

For the development of high energy storage density capacitors, a linear dielectric that possesses a high permittivity, high resistivity, and high dielectric breakdown strength is desirable. For emerging applications, such as advanced electric drive technologies, these materials must withstand extreme conditions such as a high electric field and high temperatures. High permittivity capacitor materials are generally derived from perovskite structures, for example, barium titanate ($BaTiO_3$) ceramics. The dielectric properties of $BaTiO_3$ can be manipulated through doping or through the formation of solid solutions with other perovskite compounds.[1–9] Although the dielectric characteristics have continually been improved, the deterioration of the permittivity or resistivity limits their usage under extreme conditions.

Solid solutions between Bi-perovskites and compounds such as $BaTiO_3$ and $PbTiO_3$ have resulted in unique properties, including high Curie temperatures for high temperature piezoelectric materials such as $PbTiO_3$–$Bi(Zn_{1/2}Ti_{1/2})O_3$,[10] high energy density capacitors for energy storage in $BaTiO_3$–$Bi(Zn_{1/2}Ti_{1/2})O_3$[11] and $BaTiO_3$–$BiScO_3$,[12] and temperature stable dielectrics for high temperature capacitors in $BaTiO_3$–$Bi(Zn_{1/2}Ti_{1/2})O_3$–$BiScO_3$.[13] This material has also been shown to be highly promising in multilayer embodiments for high temperature applications.[14] To achieve high energy densities and high insulation resistance at high temperatures, the defect equilibrium plays a crucial role in controlling the resistivity. Previous studies on $BaTiO_3$–$Bi(Zn_{1/2}Ti_{1/2})O_3$ ceramics showed a dramatic improvement of the insulation resistance, especially at >200 °C, upon introduction of 2 mol. % Ba vacancies into the $(Ba_{0.8}Bi_{0.2})(Zn_{0.1}Ti_{0.9})O_3$ solid solution.[15] However, the mechanisms that underpin the high insulation resistance behavior in the Ba-deficient composition $(Ba_{0.78}\square_{0.02}Bi_{0.2})(Zn_{0.1}Ti_{0.9})O_{2.98}$ ceramics are not fully understood.[16]

In this study, we demonstrate that the presence of a barium vacancy-oxygen vacancy pair in a barium titanate-based dielectric is an effective mechanism to improve the insulation resistance of dielectrics. The identification of specific defect species using an electron paramagnetic resonance (EPR) technique will be discussed. The presence of these defects, which resulted in the perturbation of the electronic structure of the material, could be also observed in the optical absorption spectra. Additionally, it will be shown that changes in the dominant defect species resulted in dramatically different conduction mechanisms in these materials.

Polycrystalline $BaTiO_3$–$Bi(Zn_{1/2}Ti_{1/2})O_3$ ceramics were prepared by a solid-state reaction technique, as described in more detail elsewhere.[16] In this technique, metal oxides and carbonates were calcined at 950 °C for 4 h and sintered at 1180 °C for 4 h in air. The stoichiometric composition, $(Ba_{0.8}Bi_{0.2})(Zn_{0.1}Ti_{0.9})O_3$, and a 2 mol. % Ba-deficient composition, specifically $(Ba_{0.78}\square_{0.02}Bi_{0.2})(Zn_{0.1}Ti_{0.9})O_{2.98}$, were batched and investigated in this study. A single perovskite phase of both compositions was observed by x-ray diffraction (D8 Discover, Bruker-AXS Inc., Madison, WI) with a Cu $K\alpha$ source in a standard Bragg-Brentano geometry. The stoichiometric composition exhibited a grain size of 8.2 ± 0.6 μm while a smaller grain size of 1.4 ± 0.04 μm was observed for the 2 mol. % Ba-deficient composition. Ceramic samples were ground into a fine powder and an EPR spectrometer (Bruker EleXsys E-500-A equipped with ER 049SX SuperX microwave bridge) was used to detect paramagnetic centers. The EPR data were obtained at 9.38 GHz (X-band) at low temperature (77 K) using a cryostat module (Oxford Instruments). In addition, optimized spectra were obtained by operating the spectrometer at 100 kHz modulation frequency, 3 G modulation amplitude, and 2.165 (20 dB) microwave power. The diffuse reflectance spectroscopic measurements were conducted at room temperature on the sintered and ground pellets over the range of 200–1100 nm using an Ocean Optics HR4000 UV-Vis spectrometer (Ocean Optics, Dunedin, FL) with a balanced deuterium/tungsten halogen source. Diffuse reflectance data were analyzed by fitting the data according to the Kubelka-Munk equation[17] and, subsequently, Tauc equation,[18] which reveals absorption characteristics near the band edge. For electrical measurements, silver electrodes were applied on the parallel surfaces of disk shaped samples. The resistivity of the material was characterized via

TABLE I. Paramagnetic centers in pure and doped $BaTiO_3$ and related materials with their g-factors as observed using EPR spectroscopy.

Paramagnetic center	g-factor	Temperature (K)	Reference
$Ti^{3+} - V_O$	1.963	300 K	19
	1.920–1.937	10–80 K	20
Ti^{3+}	1.906	20 K	21
	1.900	77 K	22
$V_{Ba} - V_O^{\bullet}$	2.005	77 K	22 and 23
V'_{Ba}	1.997	300 K	19
Co^{2+}	4.341	17 K	24
Fe^{3+}	2.00	298 K	26
$Fe^{3+} - V_O^{\bullet\bullet}$	3.955	20 K	25
Mn^{2+}	2.0024	300 K	19
	2.000	<202 K	23
Cr^{3+}	1.971-1.974	290 K	21
	1.970	77 K	22
	1.975	<202 K	23

impedance spectroscopy over the frequency range 10^{-1} to 10^6 Hz. The impedance measurements were conducted over the temperature range 623–863 K after the sample was equilibrated for an hour at the measurement temperature by using a Solartron SI1260A impedance/gain-phase analyzer equipped with a Solartron 1296A dielectric interface (Solartron Analytical, Farnborough, UK). The impedance measurements are described in more detail in Ref. 16.

The main focus of this work is to understand the interrelationship(s) among non-stoichiometry, defect equilibria, and transport properties in perovskite solid solutions based on $BaTiO_3$–$Bi(Zn_{1/2}Ti_{1/2})O_3$. The EPR technique has been used to investigate defect species in perovskite materials through the detection of paramagnetic center. A number of defect species have been previously identified by EPR in $BaTiO_3$, as listed in Table I.

In this study, the X-band EPR spectra showed a significant difference between the stoichiometric composition (S) and the Ba-deficient composition (−2Ba), as shown in Fig. 1. A weak singlet signal at g = 4.234 was observed in both the S and −2Ba samples that is likely due to Co^{2+} ions[24] which exist as known impurities in the starting materials. For the S sample, two signals were observed, one at $g = 2.0067 \pm 0.0002$ and another at $g = 1.9599 \pm 0.0005$. However, in the −2Ba sample only the signal at $g = 2.0061 \pm 0.0001$ was observed. Furthermore, the magnitude of the signal at g = 2.0061 observed in the −2Ba sample was significantly stronger than that for the S sample (g = 2.0067). The amplitude of the EPR signal for the S sample was enhanced (×10) in Fig. 1 for clarification purposes. The line widths obtained from the singlet signal at g = 2.0061 and g = 1.9599 were 4.3 G and 7.1 G, respectively.

For the stoichiometric (S) composition, the paramagnetic center at g = 1.9599 clearly originated from the presence of Ti^{3+}-related defect centers.[27,28] These defect states are commonly observed in $BaTiO_3$ processed under reducing conditions. For the paramagnetic centers at g = 2.0067 and 2.0061 observed in the S and −2Ba samples, respectively, it most likely originated from the defect associate $(V''_{Ba} - V_O^{\bullet})'$ as proposed by Jida and Miki.[23] This paramagnetic active defect is characterized by an electron trapped inside a barium vacancy-oxygen vacancy pair $(V''_{Ba} - V_O^{\bullet\bullet})$. The signal at g = 2.0061-2.0067 observed in this study was not exactly the same as the signal observed at g = 2.005 in Ref. 23. However, there are some important differences between the compositions in our study and those in Jida's work. Jida's work identified the defect associate $(V''_{Ba} - V_O^{\bullet})'$ in Nb-doped $BaTiO_3$, whereas the composition in this study was pseudo-cubic and included 20% Bi on the A-site and 10% Zn on the B-site. It is unlikely that the signal at g = 2.0061-2.0067 originated from Mn^{2+} or Fe^{3+} where the g-value is expected to be closer to $g \approx 2.00$.[24,26] Due to the hyperfine splitting of the nuclear spin in Mn^{2+} (I = 5/2),[24,26] six sharp peaks would be expected instead of one sharp signal. This behavior was not observed in the data in this study. In addition, Fe^{3+}, which is often found as an impurity in titanate perovskites, could also induce a signal near $g \approx 2.00$.[26] However, the same precursor reagents were used for both the stoichiometric and non-stoichiometric compositions in this study, and if the signal at g = 2.0061-2.0067 originated from the Fe^{3+} there should be no difference in the observed signal intensity for

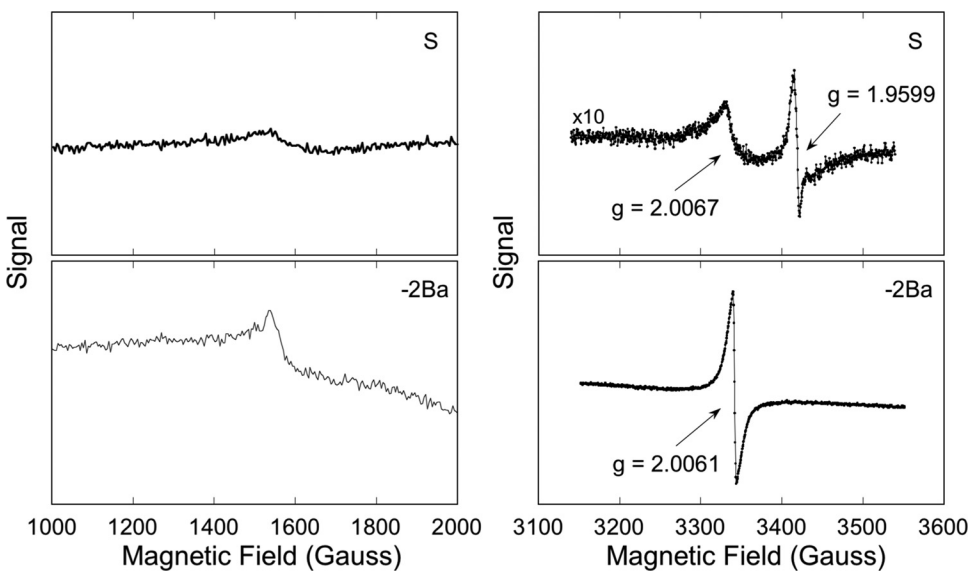

FIG. 1. X-band (9.38 GHz) electron paramagnetic resonance spectra of S and −2Ba BT-BZT ceramics measured at 77 K.

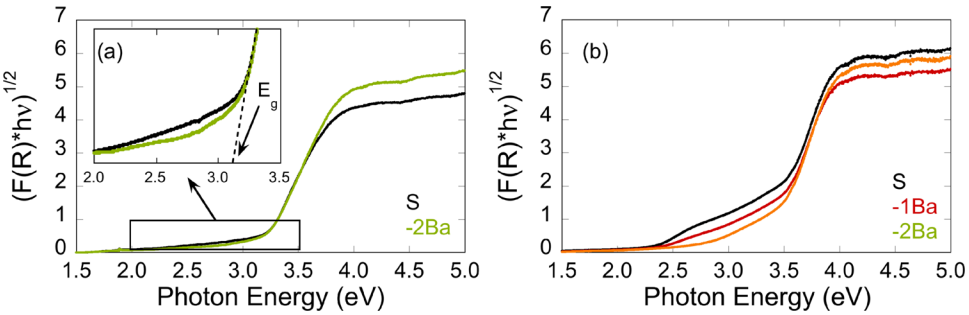

FIG. 2. Tauc plot showing optical absorption near band edge for (a) 80BT-20BZT and (b) 50BT-25BZT-25BS ceramics.

both compositions. Therefore, the data strongly suggest that the signal at g = 2.0061–2.0067 should be assigned to the defect associate $(V''_{Ba} - V^{\bullet}_{O})'$ rather than Mn^{2+} or Fe^{3+}.

Optical absorption of the stoichiometric (S) and the 2 mol. % Ba-deficient (−2Ba) compositions is shown in Figure 2. The optical band gap estimated by extrapolation to where the absorption is zero is shown in the inset of Figure 2(a). The (indirect) optical band gaps of the S and −2Ba samples were 3.16 and 3.17 eV, respectively. These values are comparable to that of $BaTiO_3$ and $SrTiO_3$ (3.2 eV),[29] and their solid solutions with, e.g., $CaTiO_3$, $BaZrO_3$, and $CaZrO_3$.[30,31] Band-to-band transitions in titanate perovskite are mainly dominated by transitions from O 2*p* states (top of valence band) to Ti 3*d* states (bottom of conduction band), which can be seen in a number of first principle calculations.[32,33] In this study, the perovskite solid solutions are composed of 80% $BaTiO_3$ and 20% $Bi(Zn_{1/2}Ti_{1/2})O_3$, which means 10% of the B-sub-lattice includes Zn ion substitutions for Ti and 20% of the A sub-lattice includes Bi ion substitutions for Ba. A perturbation of the electron wave functions of Ti 3*d* states is thus expected to occur in the system. One important feature was observed in the absorption spectrum near the band edge. This feature in the photon energy range of 2.5–3.2 eV (Urbach region) was much more prominent in the stoichiometric sample as compared to the Ba-deficient sample (Fig. 2(a)). It was proposed by Sumi and Toyozawa[34] that the Urbach edge originates from exciton-phonon interactions. Another model for the Urbach edge proposed by Cody *et al.*[35] states that it originates from thermal and structural disorder. A number of studies on different materials, including $BaTiO_3$, have shown that the Urbach edge originates from thermal and structural disorder.[30,34–38] A study by Scharfschwerdt *et al.*[20] showed that the $(Ti'_{Ti} - V^{\bullet\bullet}_{O})$ type defect centers in $BaTiO_3$ become populated after illumination with photon energies greater than 2.5 eV. The observed absorption at a photon energy >2.5 eV in the stoichiometric sample in this study could be attributed to the presence of $(Ti'_{Ti} - V^{\bullet\bullet}_{O})$ defect centers, as observed in EPR spectra. A lack of $(Ti'_{Ti} - V^{\bullet\bullet}_{O})$ defect centers in the Ba-deficient composition led to the reduced absorption near the band edge, as seen in Fig. 2(a). Furthermore, the optical spectra showed a similar observation of reduced absorption in the Urbach edge region in the 2 mol. % Ba-deficient composition of the ternary $BaTiO_3$-$Bi(Zn_{1/2}Ti_{1/2})O_3$-$BiScO_3$ system, as shown in Fig. 2(b). Based on these findings, a similar mechanism is expected in this ternary system.

The conductivity of the S and −2Ba (80BT-20BZT) samples was measured at high temperatures (623–863 K) using impedance spectroscopy. This characterization technique was used to measure the electrical properties of the polycrystalline microstructure and to determine whether homogeneous or heterogeneous electrical characteristics existed. In other words, the electrical heterogeneity originating from individual bulk, grain boundary, and electrode contributions could be isolated by this technique. The dispersion of the imaginary impedance (Z″) and imaginary modulus (M″) at selected temperatures (653, 753, and 863 K) is shown in Fig. 3. In the stoichiometric composition, multiple relaxation peaks could be observed at all measurement temperatures, as seen from the Z″ data, which indicates an electrically heterogeneous microstructure. In contrast, in the −2Ba sample, a single relaxation peak was observed over all measure temperatures, which indicates an electrically homogeneous microstructure.

The conductivity of the stoichiometric composition (S), which exhibited an electrically heterogeneous microstructure, could be attributed to bulk and grain boundary elements with activation energies of 1.17 and 1.43 eV, respectively, as shown in Fig. 4. The conductivity of the 2 mol. % Ba-deficient composition (−2Ba), in contrast, which exhibited an electrically homogeneous microstructure, could be attributed mainly to the bulk with the activation energy of 1.61 eV. Additionally, the −2Ba sample was characterized by a significantly lower conductivity compared to that of the

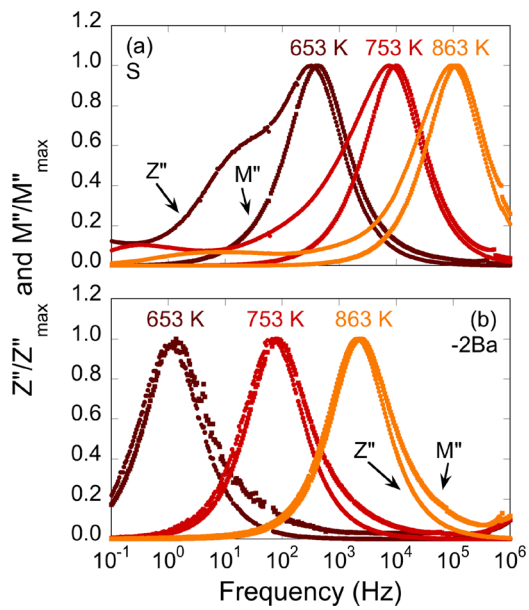

FIG. 3. Frequency dependence of imaginary impedance (Z″) and imaginary modulus (M″) of (a) the stoichiometric and (b) the 2 mol. % Ba-deficient compositions measured at 653, 753, and 863 K.

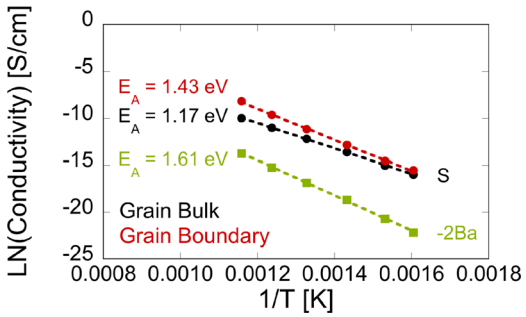

FIG. 4. Arrhenius plot of conductivity obtained from impedance measurement of S (both grain and grain boundary) and −2Ba BT-BZT ceramics measured at 623–863 K.

S sample. For example, at 653 K, the conductivity of the −2Ba sample was 1.0×10^{-9} S/cm compared to 7.9×10^{-7} S/cm for the S sample.

For the stoichiometric composition, the activation energy of 1.17 eV could be related to the presence of oxygen vacancy defect species in the bulk, via;[9,39–41]

$$O_O^x \rightarrow V_O^{\bullet\bullet} + 2e' + \frac{1}{2}O_2(g). \quad (1)$$

The oxygen loss during firing at high temperatures generates free electrons in the system, which could be trapped at Ti sites leading to the reduction of Ti^{4+}, via;

$$Ti^{4+} + e' \rightarrow Ti^{3+}. \quad (2)$$

This could be an explanation of the signal related to the Ti^{3+}-related defect centers observed in the EPR data. It could also lead to the observation of relatively high conductivities in the S sample compared to that of the −2Ba sample. It should be noted that the conduction from small-polaron hopping process was considered and found not to be consistent with our data. The origin of the higher activation energy of 1.43 eV in the grain boundary component might be attributed to a conduction mechanism that requires higher energies than that of oxygen vacancies, which could include an ionic conduction mechanism. Barium vacancies are known to exist in semiconducting $BaTiO_3$ specifically in the vicinity of grain boundaries due to re-oxidation processes.[42,43] Recall that the impedance data for the S sample clearly indicated an electrically heterogeneous microstructure, and therefore the observed weak EPR signal related to barium vacancies could come from the grain boundary region in a core-shell microstructure. This is consistent with the finding that the amplitude of the EPR signal from the Ti^{3+}-related defect center was comparatively larger than that of the barium vacancy defect.

The conductivity of the non-stoichiometric (−2Ba) sample exhibited an electrically homogeneous microstructure, which was dominated only by the bulk component with a significantly lower conductivity than that of the S sample. Given the known temperature dependence of the conductivity of a semiconductor ($\sigma = nq\mu$):

$$n_i = (\text{constant})T^{3/2}\exp(-E_g/2k_BT). \quad (3)$$

The value for E_g was obtained from fitting the conductivity data. A large activation energy of 1.61 eV was measured which indicates a band gap (E_g) of approximately 3.2 eV. This value is very close to the band gap measured by the prior optical technique (3.17 eV).

Density functional theory (DFT) calculations of the defect energies in paraelectric $BaTiO_3$, which appears to be closely relevant to the materials in this study, showed that stable $(V''_{Ba} - V_O^{\bullet\bullet})$ defect states lie close to the band edge.[44] This might support the observation of large activation energies in non-stoichiometric compositions due to the lack of intermediate states inside the band gap. Thus, high resistivities could be achieved in the Ba-deficient composition.

In conclusion, we demonstrated that the nature and type of defect species in $0.8BaTiO_3$–$0.2Bi(Zn_{1/2}Ti_{1/2})O_3$ solid solutions result in dramatically different electronic properties. Defects related to Ti^{3+} centers, observed in the stoichiometric composition, appear to be derived from the reduction of Ti^{4+} by trapped electrons that originate from oxygen loss at high temperatures. This results in an electrically heterogeneous structure, which leads to relatively high conductivity at elevated temperatures. The presence of defect associate $(V''_{Ba} - V_O^{\bullet\bullet})$ in the 2 mol. % Ba-deficient composition, which acts as an effective electron-trapping site, resulted in an electrically homogeneous structure with an increase in resistivity, especially at high temperature. This finding about the role of the defect associate $(V''_{Ba} - V_O^{\bullet\bullet})$ in $BaTiO_3$-based compounds will provide insights on the development of high energy density dielectric materials with high resistivity for demanding high temperature applications.

The authors would like to acknowledge NSF CHE-0840478 for funding the EPR spectroscopy at CAMCOR at the University of Oregon. A portion of this work was supported by the Energy Storage Program managed by Dr. Imre Gyuk of the Department of Energy's Office of Electricity Delivery and Energy Reliability. Sandia National Laboratories is a multi-program laboratory managed and operated by Sandia Corporation, a wholly owned subsidiary of Lockheed Martin Corporation, for the U.S. Department of Energy's National Nuclear Security Administration under contract DE-AC04-94AL85000.

[1]R. Guo, L. E. Cross, S.-E. Park, B. Noheda, D. E. Cox, and G. Shirane, Phys. Rev. Lett. **84**, 5423 (2000).
[2]W. Liu and X. Ren, Phys. Rev. Lett. **103**, 257602 (2009).
[3]G. H. Haertling, J. Am. Ceram. Soc. **82**, 797 (1999).
[4]J. Rodel, W. Jo, K. T. P. Seifert, E.-M. Anton, T. Granzow, and D. Damjanovic, J. Am. Ceram. Soc. **92**, 1153 (2009).
[5]D. C. Sinclair and A. R. West, J. Appl. Phys. **66**, 3850 (1989).
[6]T. Tsurumi, H. Adachi, H. Kakemoto, S. Wada, Y. Mizuno, H. Chazono, and H. Kishi, Jpn. J. Appl. Phys. Part 1 **41**, 6929 (2002).
[7]D. E. McCauley, M. S. H. Chu, and M. H. Megherhi, J. Am. Ceram. Soc. **89**, 193 (2006).
[8]I. Levin, E. Cockayne, V. Krayzman, J. C. Woicik, S. Lee, and C. A. Randall, Phys. Rev. B **83**, 094122 (2011).
[9]F. D. Morrison, D. C. Sinclair, and A. R. West, J. Appl. Phys. **86**, 6355 (1999).
[10]I. Grinberg, M. R. Suchomel, W. Dmowski, S. E. Mason, H. Wu, P. K. Davies, and A. M. Rappe, Phys. Rev. Lett. **98**, 107601 (2007).
[11]C. C. Huang and D. P. Cann, J. Appl. Phys. **104**, 024117 (2008).
[12]H. Ogihara, C. A. Randall, and S. Trolier-McKinstry, J. Am. Ceram. Soc. **92**, 1719 (2009).
[13]C. C. Huang, D. P. Cann, X. Tan, and N. Vittayakorn, J. Appl. Phys. **102**, 044103 (2007).
[14]N. Raengthon, T. Sebastian, D. Cummings, I. M. Reaney, and D. P. Cann, "$BaTiO_3$–$Bi(Zn_{1/2}Ti_{1/2})O_3$–$BiScO_3$ Ceramics for High-Temperature Capacitor Applications," J. Am. Ceram. Soc.

[15]N. Raengthon and D. P. Cann, IEEE Trans. Ultrason. Ferroelectr. Freq. Control **58**, 1954 (2011).
[16]N. Raengthon and D. P. Cann, J. Am. Ceram. Soc. **95**, 1604 (2012).
[17]J. D. Lindberg, Appl. Opt. **26**, 2900 (1987).
[18]J. Tauc, R. Grigorovici, and A. Vancu, Phys. Status Solidi B **15**, 627 (1966).
[19]N. S. Hari, P. Padmini, and T. R. N. Kutty, J. Mater. Sci. Mater. Electron. **8**, 15 (1997).
[20]R. Scharfschwerdt, A. Mazur, O. F. Schirmer, H. Hesse, and S. Mendricks, Phys. Rev. B **54**, 15284 (1996).
[21]V. V. Laguta, A. M. Slipenyuk, I. P. Bykov, M. D. Glinchuk, M. Maglione, A. G. Bilous, O. I. V'yunov, J. Rosa, and L. Jastrabik, J. Appl. Phys. **97**, 073707 (2005).
[22]Y. Uchida, A. Kai, T. Murata, and T. Miki, Jpn. J. Appl. Phys. Part 1 **43**, 669 (2004).
[23]S. Jida and T. Miki, J. Appl. Phys. **80**, 5234 (1996).
[24]R. N. Schwartz and B. A. Wechsler, Phys. Rev. B **48**, 7057 (1993).
[25]W. L. Warren, D. Dimos, G. E. Pike, and K. Vanheusden, Appl. Phys. Lett. **67**, 1689 (1995).
[26]G. Er, S. Ishida, and N. Takeuchi, J. Mater. Sci. **34**, 4265 (1999).
[27]T. Kolodiazhnyi and A. Petric, J. Phys. Chem. Solid **64**, 953 (2003).
[28]R. A. Eichel, Phys. Chem. Chem. Phys. **13**, 368 (2011).
[29]M. Cardona, Phys. Rev. **140**, A651 (1965).
[30]S. Lee, R. D. Levi, W. Qu, S. C. Lee, and C. A. Randall, J. Appl. Phys. **107**, 023523 (2010).
[31]S. Lee, W. H. Woodford, and C. A. Randall, Appl. Phys. Lett. **92**, 201909 (2008).
[32]A. Chassé, St. Borek, K.-M. Schindler, M. Trautmann, M. Huth, F. Steudel, L. Makhova, J. Gräfe, and R. Denecke, Phys. Rev. B **84**, 195135 (2011).
[33]S. Saha, T. P. Sinha, and A. Mookerjee, Phys. Rev. B **62**, 8828 (2000).
[34]H. Sumi and Y. Toyozawa, J. Phys. Soc. Jpn. **31**, 342 (1971).
[35]G. D. Cody, T. Tiedje, B. Abeles, B. Brooks, and Y. Goldstein, Phys. Rev. Lett. **47**, 1480 (1981).
[36]S. Knief and W. von Niessen, Phys. Rev. B **59**, 12940 (1999).
[37]T. He, P. Ehrhart, and P. Meuffels, J. Appl. Phys. **79**, 3219 (1996).
[38]K.-D. Becker, M. Schrader, H.-S. Kwon, and H.-I. Yoo, Phys. Chem. Chem. Phys. **11**, 3082 (2009).
[39]R. Waser, T. Baiatu, and K. H. Hardtl, J. Am. Ceram. Soc. **73**, 1645 (1990).
[40]C. Ang, Z. Yu, and L. E. Cross, Phys. Rev. B **62**, 228 (2000).
[41]O. Raymond, R. Font, N. Suarez-Almodovar, J. Portelles, and J. M. Siquerios, J. Appl. Phys. **97**, 084107 (2005).
[42]R. Huybrechts, K. Ishizaki, and M. Takata, J. Mater. Sci. **30**, 2463 (1995).
[43]J. Daniels and R. Wernicke, Philips Res. Rep. **31**, 544 (1976).
[44]P. Erhart and K. Albe, J. Appl. Phys. **102**, 084111 (2007).